# 2-Dimensional Analytic Approach for Anion Differentiation using Chromo-Fluorogenic Receptors

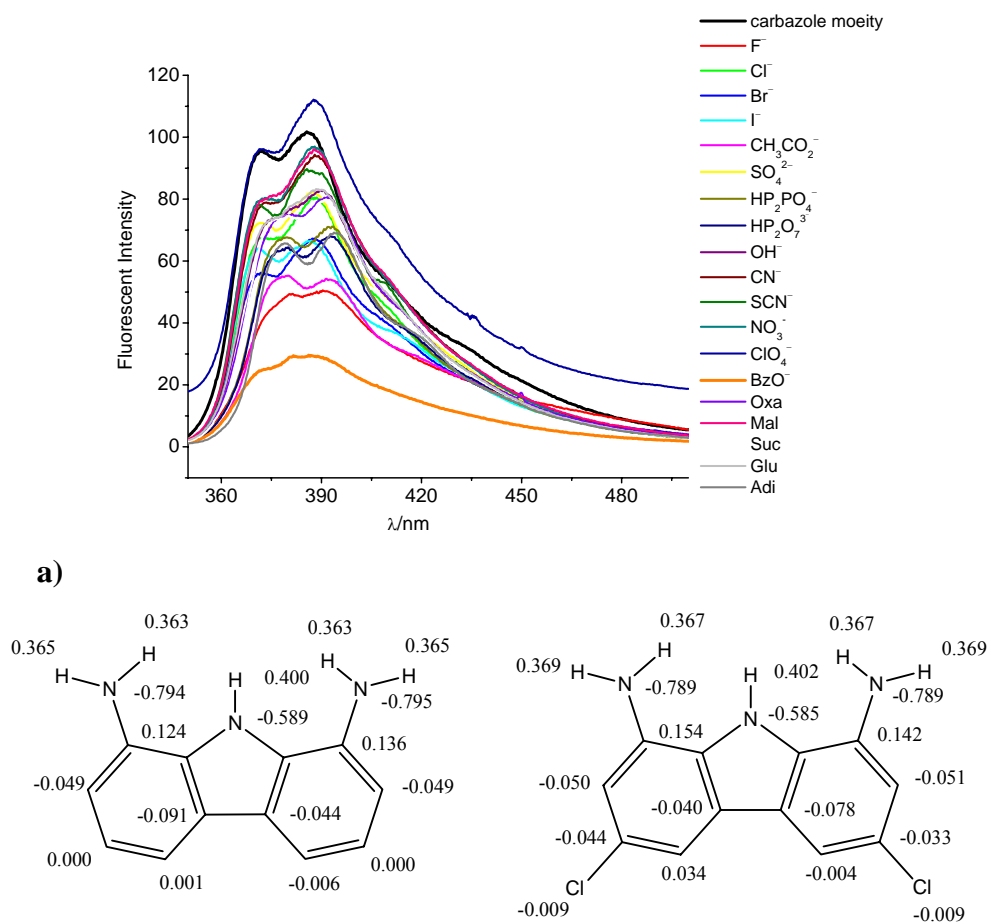T. Daniel Thangadurai, N. Jiten Singh, In-Chul Hwang, Jung Woo Lee, R. Prakash Chandran, Kwang S. Kim*

Center for Superfunctional Materials, epartment of Chemistry
Pohang University of Science and Technology
Pohang 790-784, Korea

**Supporting Information  - II**

## I. Toward the Design Approach

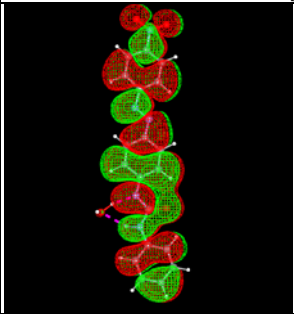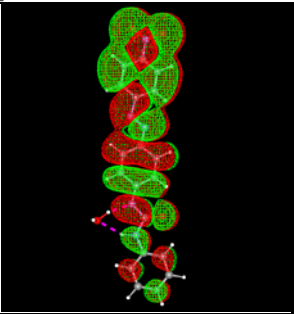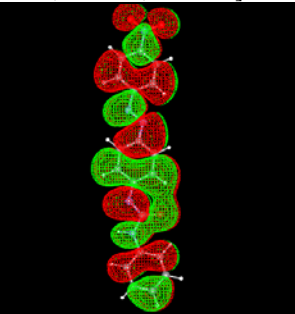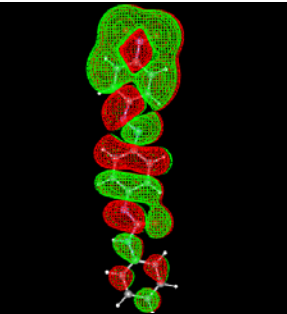**I.1**. The Fluorophore moiety (1,8-diamino-3,6-dichlorocarbazole, **F**)



a)



b)
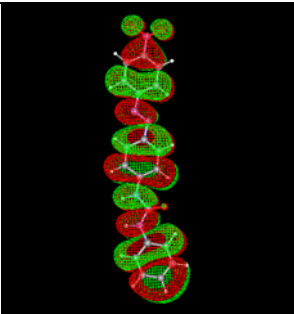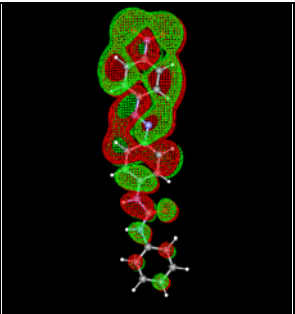
**Fig. S1.** a) Fluorescent intensity changes of 1,8-diamino-3,6-dichlorocarbazole (**F**) (10 μM, CH₃CN:DMSO 9:1 v/v) upon the addition of 100 eq. of various anions. All anions except $ClO_4^-$ show quenching in the fluorescent intensity. $BzO^-$ shows the maximal quenching effect. Therefore, virtually all the anions tested affect the fluorescent intensity of the 1,8-diamino-3,6-dichlorocarbazole; b) Natural Bond Orbital (NBO) atomic charges (B3LYP/6-311+G*) of the 1,8-diaminocarbazole and 1,8-diamino-3,6-dichlorocarbazole.The partial charges of the pyrrole H and amino H atoms in 1,8-diaminocarbazole increase slightly by 0.003 upon the 3,6-dichloro substitution. However, the 1,8-diamino-3,6-dichlorocarbazole acetate complex is found to be ~ 8 kcal/mol more stable in the gas phase than the unsubstituted counterpart. Therefore, the 3,6-dichloro substitution on 1,8-diaminocarbazole enhances the binding affinity toward anions due to the dipole enhancement, as noted in our previous work of the charge-dipole enhancement toward the anion binding [H. Ihm, S. Yun, H. G. Kim, J. K. Kim, K. S. Kim, *Org. Lett.* **2002,** *4*, 2897-2900].

**I.2** The Chromophore moiety (1-[4-(4-nitro-phenylazo)-phenyl]-3-phenyl-urea, **C**)
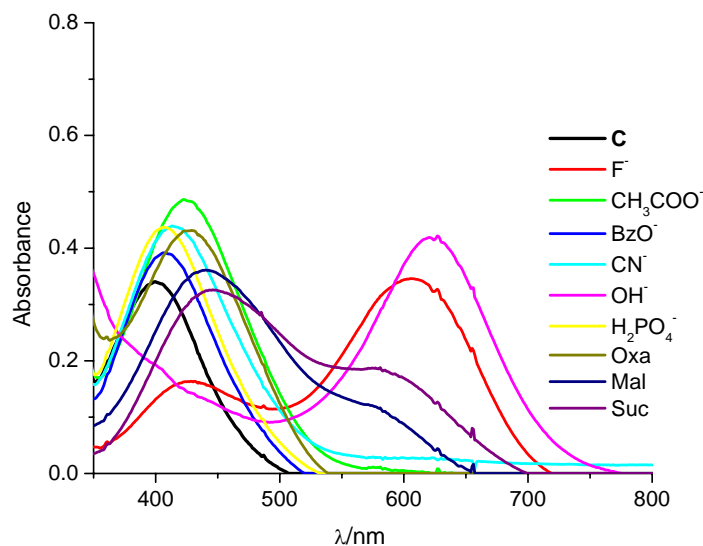


a)

**Fig. S2.** Absorbance spectra of receptor **C** (0.075 mM) upon the addition of various anions (7.5 mM) as 1:100 equivalent ratio in $CH_3CN$:DMSO (9:1, v/v). $F^-$, $OH^-$, malonate (Mal) and succinate (Suc) shows an extra peak ~590-625 nm (with the appearance of blue color in the solution), while other anions (tested here) show red shifts with respect to the 400 nm peak of **C**. Therefore, various anions would make red shifts against the 400 nm absorption peak of **C** or/and an extra peak at ~600 nm with the appearance of blue color in the solution.

**Table S1.** TDDFT/B3LYP/6-311+G* (and TDDFT/B3LYP/6-31G*) calculated important transitions for the **C** moiety, the **C**-OH complex and the **C**⁻ moiety.

| TD//B3LYP/6-311+G* | | | |
|---|---|---|---|
| |  |  | |
| | **C** HOMO (94) | **C** LUMO (95) | |
| 94 => 95, 2.79eV, 444 nm, f=0.81<br>93 => 95, 3.26 eV 380 nm, f=0.36<br>Average value = 412 nm<br>[TD/B3LYP/6-31G*: average value :404 nm]<br>[Zindo//B3LYP/6-311+G*: 67 => 68, 401 nm, f=1.28]<br>[Zindo//B3LYP/6-31G*: 67 => 68, 409 nm, f=1.28 ] | | | |
|  |  |  |  |
| **C**-OH⁻ HOMO (99) | **C**-OH⁻ LUMO (100) | *C⁻ HOMO (94) | C⁻ LUMO (95) |
| 99 => 100, 2.09eV, 591 nm, f=1.31<br>99 => 101, 2.95eV, 419 nm, f=0.48<br>[TD/B3LYP/6-31G*: 566 nm (99 => 100, f=1.29)<br>and 404 nm (99 => 101, f =0.49)]<br>[Zindo//B3LYP/6-311+G*: 71 => 72, 597 nm, f=1.66<br>71 => 73, 416 nm, f=0.12]<br>[Zindo//B3LYP/6-31G*: 71 => 72, 602 nm, f=1.68<br>71 => 73, 417 nm, f=0.11] | | 94 => 95, 2.11eV, 586 nm, f=1.43<br>94 => 96, 2.95eV, 421 nm, f=0.28<br>[TD/B3LYP/6-31G*: 561 nm (94 => 95, f=1.44)<br>and 407 nm (94 => 96, f =0.40)]<br>[Zindo//B3LYP/6-311+G*: 67 => 68, 610 nm, f=1.72<br>67 => 69, 421 nm, f=0.12]<br>[Zindo//B3LYP/6-31G*: 67 => 68, 614 nm, f=1.73<br>67 => 69, 423 nm, f=0.11]<br>* The deprotonation at urea NH connected to azo-phenyl. | |
| The change in the spectral peak (nm) for the change from the neutral (**C**) to the ionic form (**C**⁻):<br>Expt: **C**: 400 => ~586-628 nm (difference of 186-228 nm),<br>TD/B3LYP/6-311+G* 412 => 586-591nm (difference of 174-179 nm)<br>TD/B3LYP/6-31G* 404 => 561-566 nm (difference of 157-182 nm)<br>Zindo/B3LYP/6-311+G*: 401 => 602-610 nm (difference of 201-209 nm)<br>Zindo/B3LYP/6-31G*: 409 => 602-614 nm (difference of 193-205 nm) | | | |

**Fig. S3.** Bond distances (in black) and Natural Bond Orbital (NBO) charges (in blue) of **C** and **C⁻**. The deprotonation of the more acidic urea leads to the charge transfer of the proton toward the electron deficient azo-nitro-benzene group accompanied by the bond transformations, i.e. -N=N- to =N-N=.
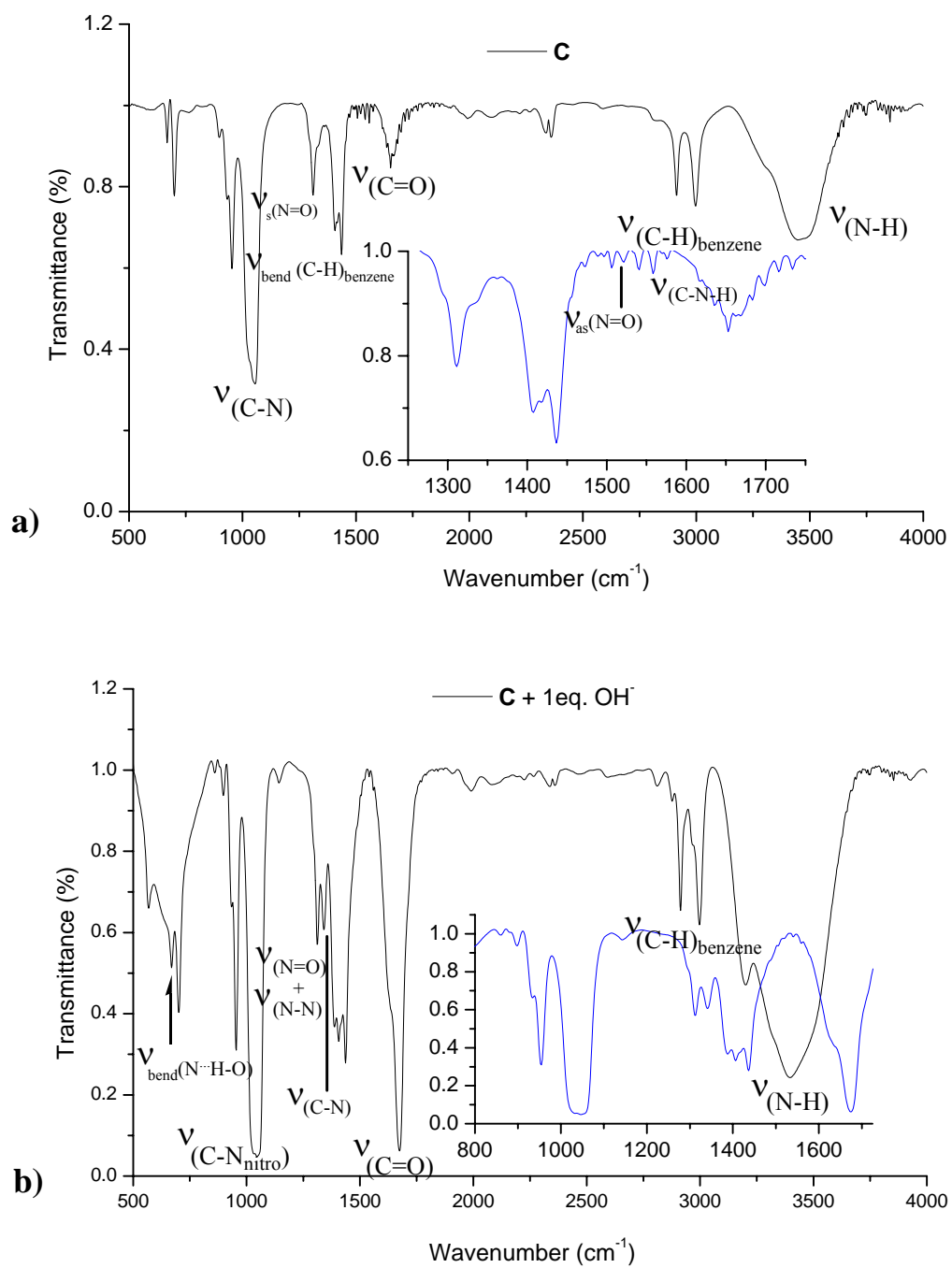
**Fig. S4.** Important characteristic IR spectra peaks of a) **C** only and b) **C** + 1 eq. OH⁻.
[**C**] = 0.075 mM; [TBA⁺OH⁻] = 0.075 mM.

**Table S2.** Important experimental and calculated IR peaks of **C** and **C**+OH⁻.

| Freq(exp) C [cm⁻¹,(Rel. Int.)] | Freq(cal)* C (cm⁻¹) | Mode |
|---|---|---|
| 1055 (1.00) | 1074 | $\nu_s$ (C−N) |
| 1309 (0.31) | 1306 | $\nu_s$ (N=O) |
| 1437 (0.53) | 1433 | benzene H bending combined with $\nu$(N=N) |
| 1506,1558 (0.04, 0.06) | 1501, 1564 | $\nu_{ben}$ (C−N−H) of more acidic urea |
| 1517, 1567 (0.02, 0.001) | 1515, 1579 | $\nu_{ben}$ (C−N−H) of less acidic urea |
| 1539 (0.05) | 1512 | $\nu_{as}$ (N=O) |
| 1651 (0.20) | 1705 | $\nu$(C=O) |
| 2912−2997(0.32, 0.36) | 3019−3127 | benzene $\nu$(C−H) |
| 3448(0.48)(b) | 3461−3476 | $\nu_s$ (N−H) |

| Freq(exp) C+OH⁻ [cm⁻¹, Rel. Int.)] | Freq(cal)* C+OH⁻ (cm⁻¹) | Mode |
|---|---|---|
| 895(0.44) | 918 | $\nu_{bend}$(N···H−O) |
| 1020 (1.00) | 1070 | $\nu_s$ (C−N) (for nitro) |
| 1311 (0.48) | 1326 | $\nu_s$ (N=O) combined with $\nu_s$ (N−N) |
| 1336 (0.32) | 1361 | $\nu_s$ (C−N) (for deprotonated N−C$_{benzene}$) |
| 1404−1435 (0.66) | 1451−61 | benzene H bending |
| − | − | $\nu_{bend}$ (C−N−H) of more acidic urea |
| − | 1522, 1568 | $\nu_{bend}$ (C−N−H) of less acidic urea |
| − | 1466 | $\nu_{as}$ (N=O) |
| 1670 (0.91) | 1705 | $\nu$(C=O) |
| − | 1566, 1584 | δ (benzene) |
| 2912−2995 (0.34, 0.42) | 3020−3124 | benzene $\nu$(C−H) |
| 3399 (0.85) | 3377 | $\nu$(N−H) |
| − | 3686 | $\nu$(O−H) |

The peaks corresponding to $\nu$(N=N) and $\nu_{bend}$(C-N-H) of more acidic urea -NH of **C** disappeared. For **C**+OH⁻, the additional peaks corresponding to $\nu_{bend}$(N…H-O) appeared distinctly. The $\nu_s$(N-N) is mixed with $\nu_{sym}$ (N=O) stretching mode. The deprotonation of the more acidic urea hydrogen in the presence of OH⁻ causes blue color (Figure S2, Table S1 and Figure S3).

## II. Experimental

All new compounds were fully characterized with standard spectroscopic techniques. Microanalyses were performed on a Carlo 1102 elemental analysis instrument. Absorption spectra were recorded using a Shanghai 756 MC UV-vis spectrometer. $^1$H NMR and $^{13}$C NMR spectra were performed on a Bruker Avance DPX500 (500 MHz) spectrometer. Infrared spectra were recorded on a Bruker Vector 22 FTIR spectrometer. High resolution mass spectra were obtained on a Micromass Platform II mass spectrometer. Fluorescent studies were performed on a Shimadzu RF-5301PC spectrofluorophotometer. Carbazole, phenyl isocyanate, naphthyl isocyanate, Disperse Orange 3 and trichloromethylchloroformate were purchased from Aldrich and used as such.

## III. Colorimetric and Absorption studies

The colorimetric studies of receptor **1** towards various anions and biological entities can be easily observed by naked eye in the $CH_3CN:DMSO$ (9:1 v/v) solution mixture at a concentration of 0.075 mM. The anions in the form of tetrabutylammonium salts in 7.5 mM concentration (with the host to guest equivalent ratio of 1:100). The solutions for the colorimetric test were used to record UV-visible absorption spectra. In the absence of anions, the spectrum of receptor **1** was characterized by the presence of two peaks at $\lambda_{max} = 360$ nm (for carbazole group), and 418 nm (for 4-isocyanato-4'-nitroazobenzene group). When the receptor solutions were exposed to anions, the absorption peak (at $\lambda_{max} = 418$ nm) was red-shifted to the visible region.
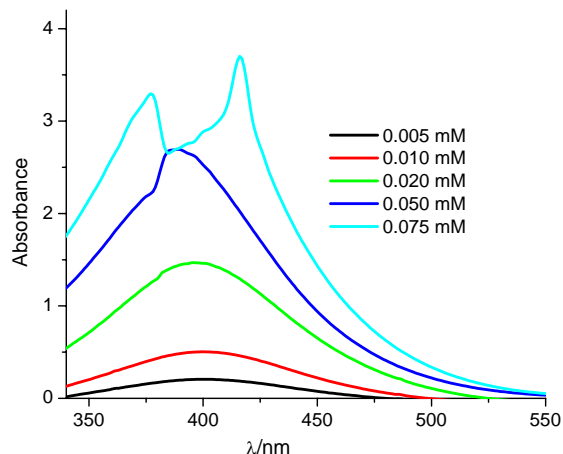
**Fig. S5.** Absorption spectra of **1** at different concentrations (0.005 mM to 0.075 mM). Till 0.05 mM, the maximum peak appears at 400 nm. However, at the noticeably naked eye detectable concentration of 0.075mM, it splits into two peaks which correspond to the excitation from the HOMO to the two LUMO states lying on the two (4-Nitro-phenyl)-phenyl-diazene arms. At lower concentrations, these two absorption peaks seem not distinguishable. We opt to use [**1**]=0.075 mM for our observation of color changes of **1** upon the addition of various anions, due to two reasons: i) Concentrations lower than 0.075 mM lead to the pale yellow color which cannot easily be noticeable by naked eyes. The color changes of **1** (0.075 mM) upon adding various anions are easily detectable by naked eyes. ii) As the two absorption peaks are split, both peaks are very sharp. The change of a sharp peak (418 nm) of **1** upon adding anions is easily observable using absorption spectrometer.

### IV. Fluorescent Studies

Fluorescent experiments were recorded at 298 K. To detect the anions, we carried out fluorescent spectrum for receptors **1**, **2** and **3** with anions in 1:100 equivalent ratio. Stock solutions of receptors **1, 2** and **3** (10 µM) and tetrabutylammonium salts of anions (1000 µM) in dry Acetonitrile/DMSO (9:1) mixture were used for the detection experiments (Fiqure S8-S10). Titration experiments were conducted by measuring the changes in fluorescence emission upon the addition of anions (10 µM for $HP_2O_7^{3-}$ and 1000 µM for $CH_3COO^-$) to the degassed 100% DMSO solution of receptors **1 & 2** (1 µM) (Fiqure S11, S12). For all

measurements, excitation was at 340 nm; emission was measured at 385 nm. For both excitation and emission, slit widths were 10 nm for receptor **1**, and 3 nm for receptors **2** and **3** with slow scan speed for detection, and 5 nm slit width was used for titration. The initial volume of all receptor solutions was 2 mL.
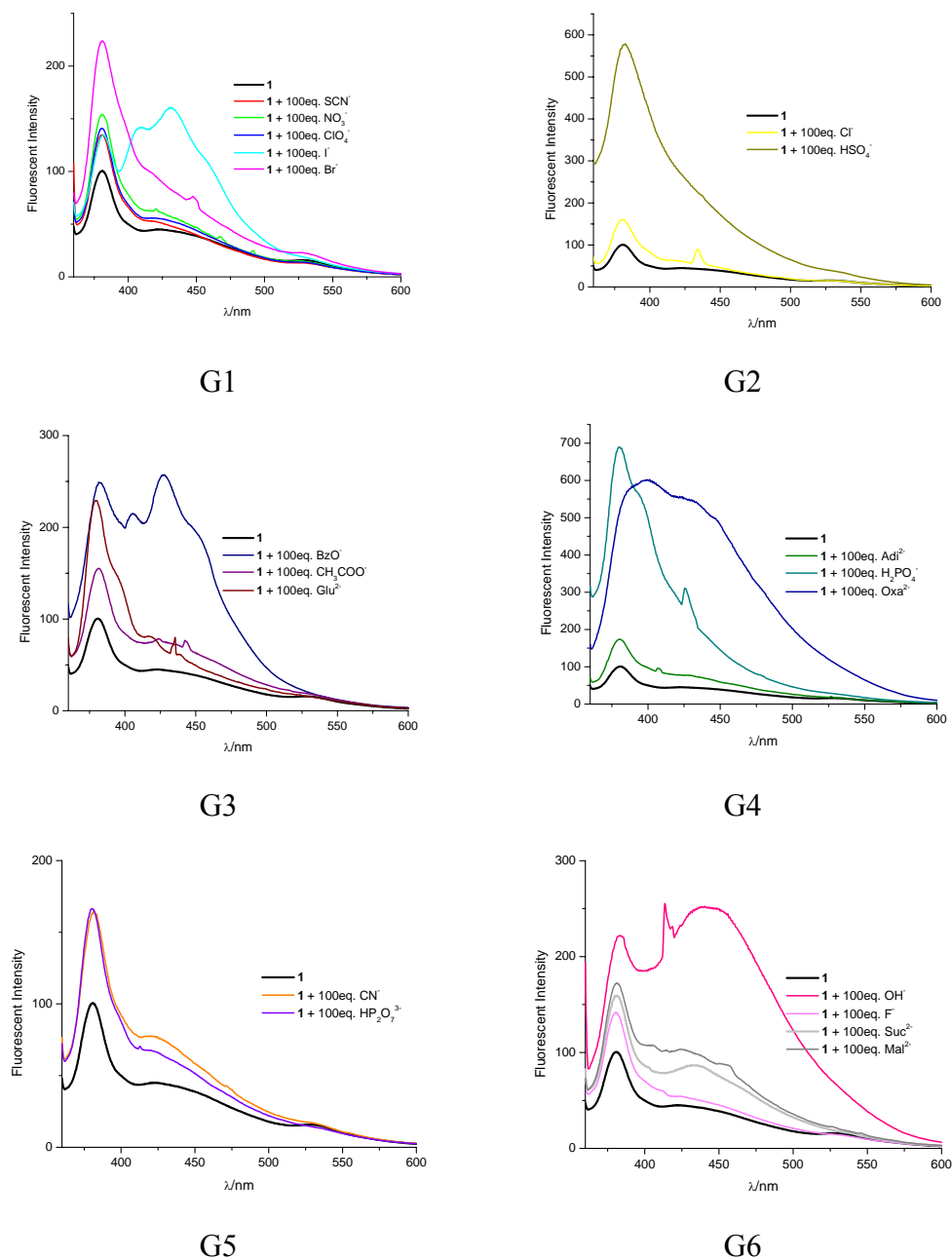


**Fig. S6-1.** Groups G1 - G6 for the fluorescence spectra of receptor **1** (10 μM) upon the addition of tetrabutylammonium salts of anions (1000 μM ) as 1:100 equivalent ratio in CH$_3$CN:DMSO (9:1, v/v) mixture (slit width = 10 nm; excitation = 340 nm).

G1



G2



G3



G4



G5



G6
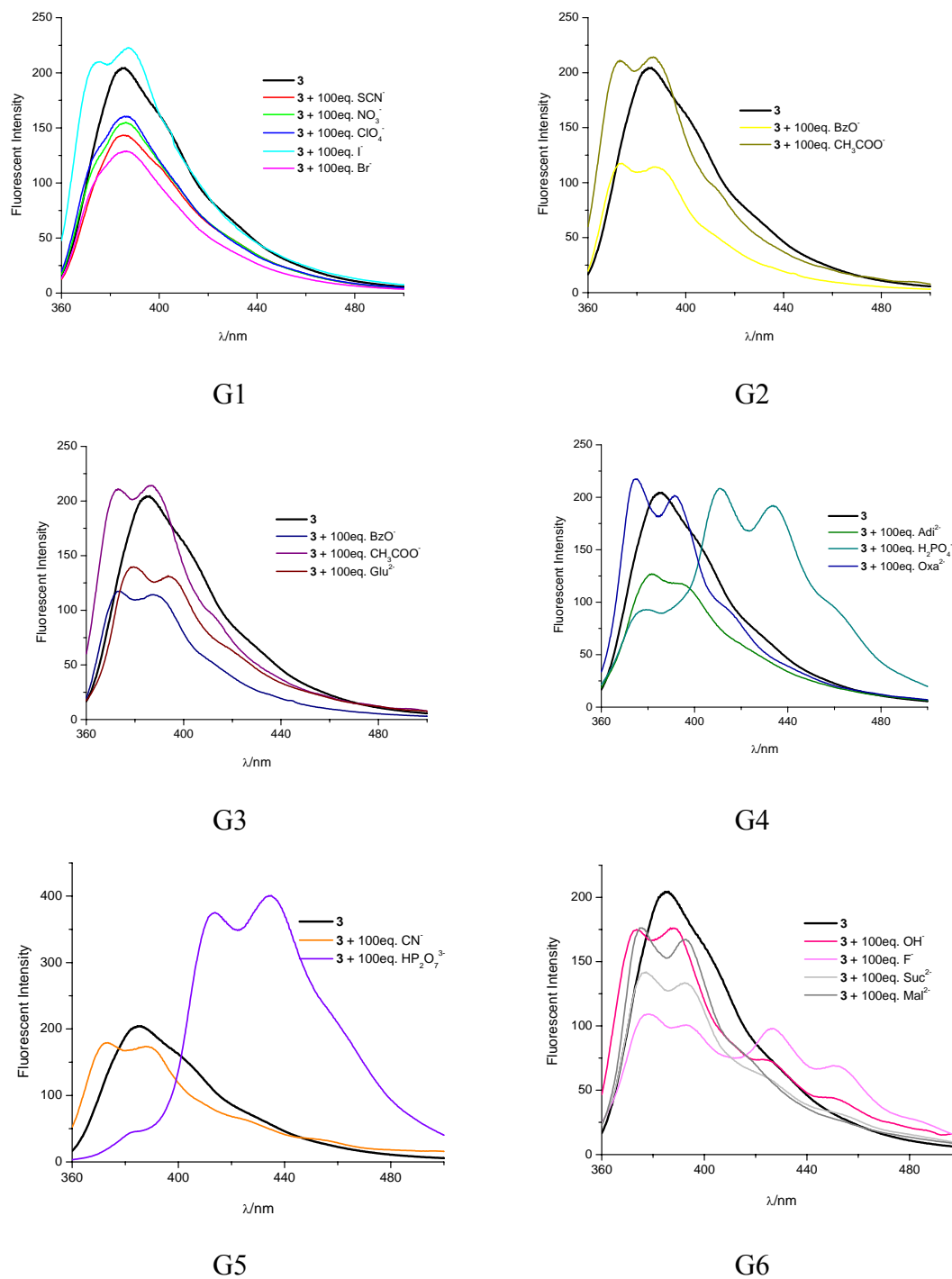
**Fig. S6-2.** Groups G1 - G6 for the fluorescence spectra of receptor **3** (10 μM) upon the addition of tetrabutylammonium salts of anions (1000 μM ) as 1:100 equivalent ratio in the CH₃CN:DMSO (9:1, v/v) mixture (slit width = 3 nm; excitation = 340 nm).

## V. $^1$H NMR Titration Studies

Proton NMR titrations were performed at 298 K. DMSO-$d_6$ was dried over molecular sieves (4 Å) before use. The anions as tetrabutylammonium salts were dried at least for a day in dynamic vacuum, prior to the experiments. The anion binding properties of receptors **2** towards various anions such as F$^-$, CH$_3$COO$^-$ and HP$_2$O$_7^{3-}$ were made using $^1$H NMR titration in DMSO-$d_6$ by monitoring the changes in the chemical shift of -NH proton of the urea moiety attached to the carbazole. The solution of receptor as 0.001 M in DMSO-$d_6$ was titrated by adding known quantities of concentrated solution of anions (0.004 M) in the form of their tetrabutylammonium salts. Every titration was repeated at least twice till consistent values were obtained (Figures S13-S15).

**V-1.** Titration of **2** with F⁻ in DMSO-$d_6$
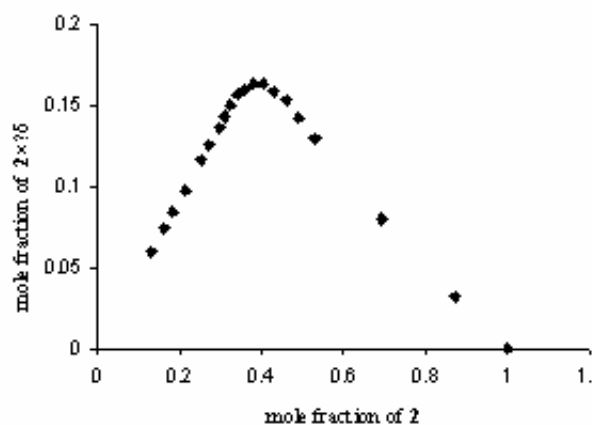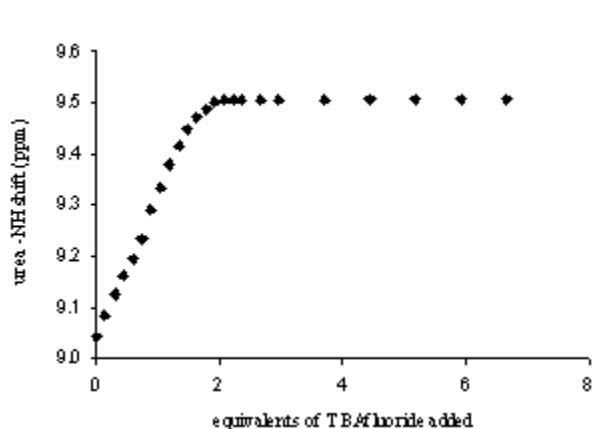




**Fig. S7-1** ¹H NMR titration curve for the receptor **2** and Fluride ion in DMSO-$d_6$.

[**2**] =1.1×10⁻³ M as the starting concentration. [TBAF]= 0–2.62×10⁻³ M.

**Fig. S7-2** Job plot for the binding of **2** and F⁻ in DMSO-$d_6$.
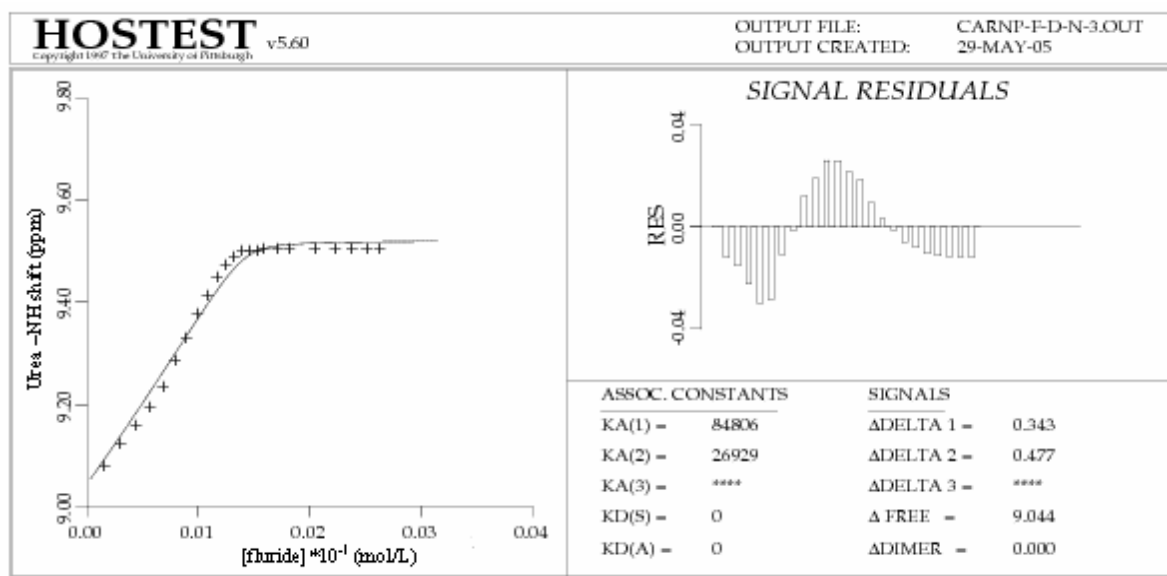


Fig. S7-3 Theoretical curve fitting. The curve shows the fit of the experimental data to a 1:2 binding profile.

**V-2.** Titration of **2** with $CH_3COO^-$ in DMSO-$d_6$
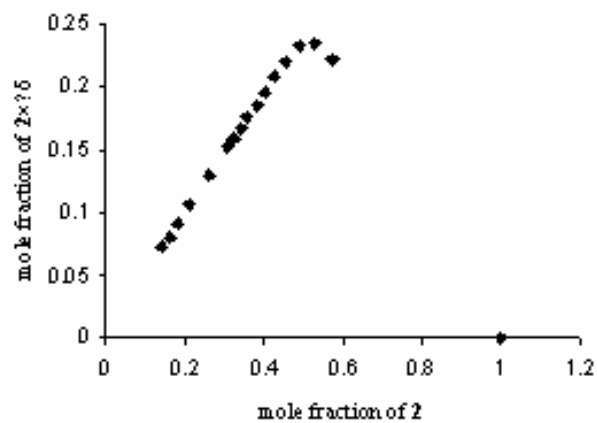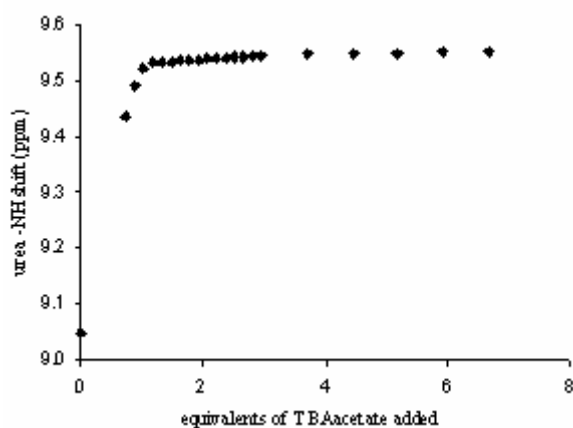




**Fig. S8-1** ^{1}H NMR titration curve for the receptor **2** and acetate ion in DMSO-$d_6$.

[**2**] =1.1×10$^{-3}$ M as the starting concentration.

[TBAacetate]= 0–2.62×10$^{-3}$ M.

**Fig. S8-2** Job plot for the binding of **2** and acetate in DMSO-$d_6$.
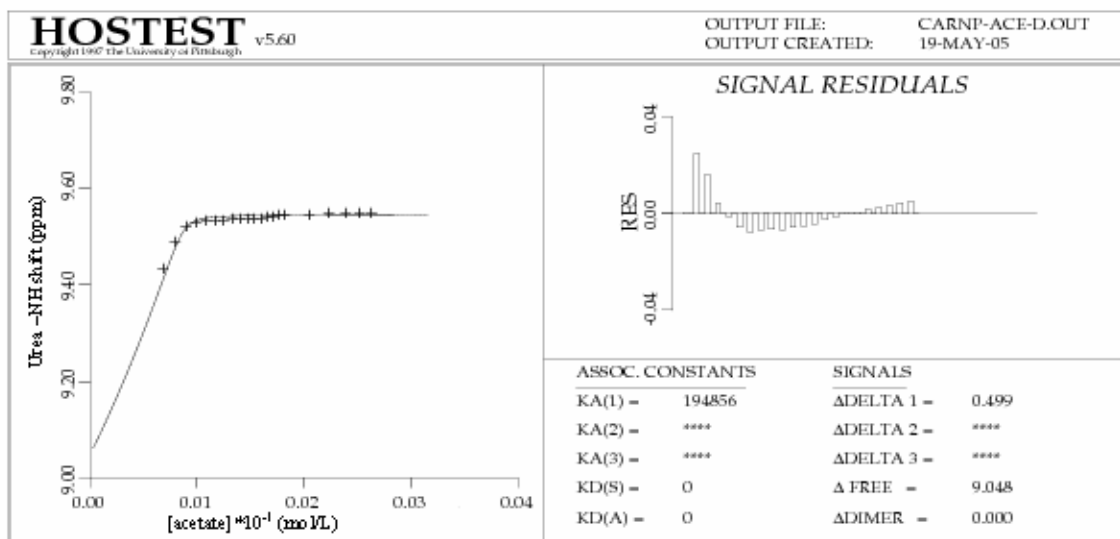


Fig. S8-3 Theoretical curve fitting. The curve shows the fit of the experimental data to a 1:1 binding profile.

**V-5.** Titration of **2** with $HP_2O_7{}^{3-}$ in DMSO-$d_6$
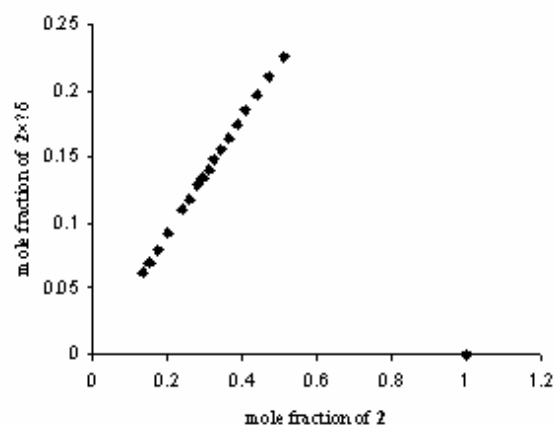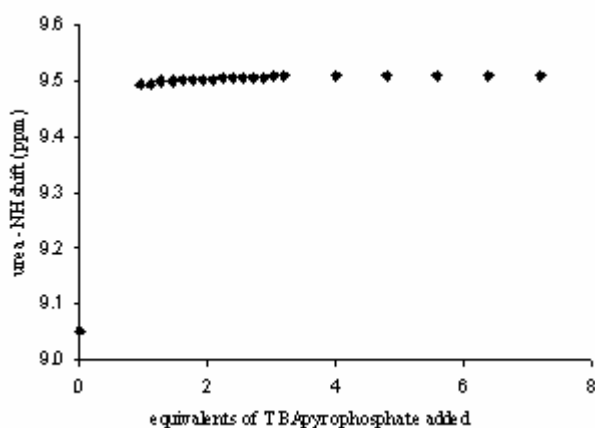




**Fig. S9-1** $^1$H NMR titration curve for the receptor **2** and pyrophosphate ion in DMSO-$d_6$.
[**2**] $=1.1\times10^{-3}$ M as the starting concentration.
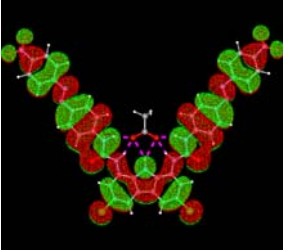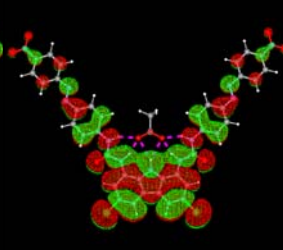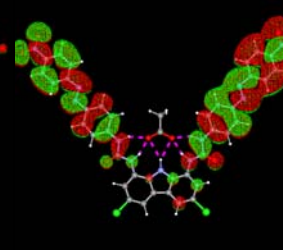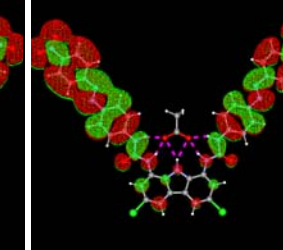[TBApyrophosphate]= $0-1.41\times10^{-3}$ M.
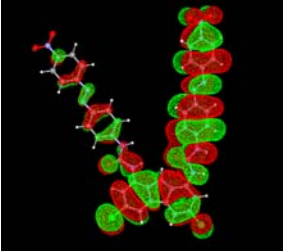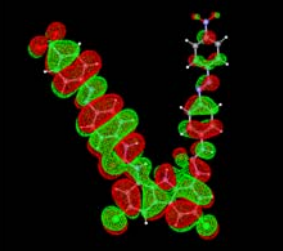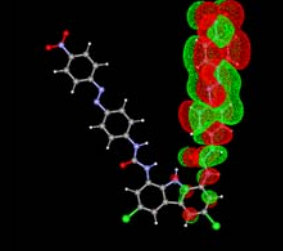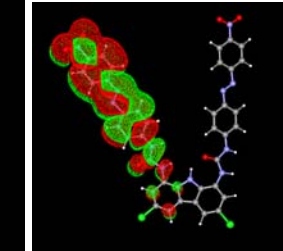
**Fig. S9-2** Job plot for the binding of **2** and pyrophosphate in DMSO-$d_6$.
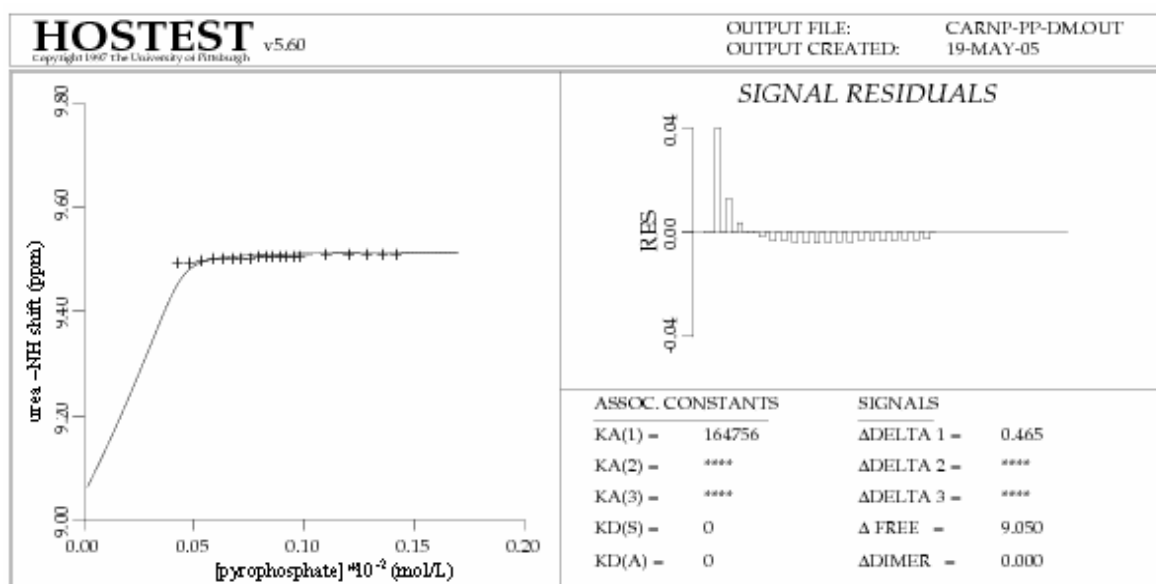


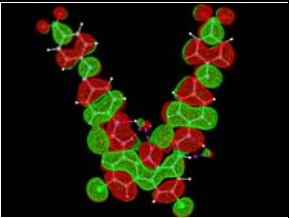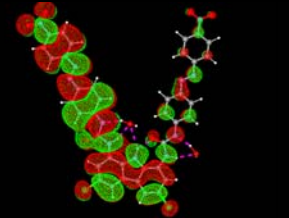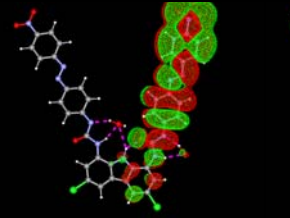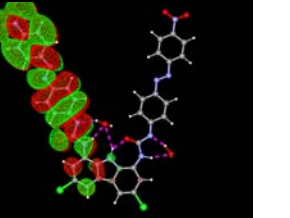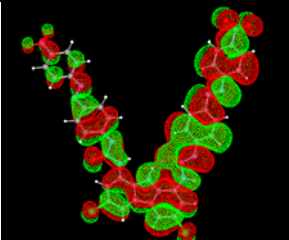Fig. S9-3 Theoretical curve fitting. The curve shows the fit of the experimental data to a 1:1 binding profile.
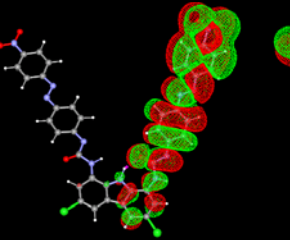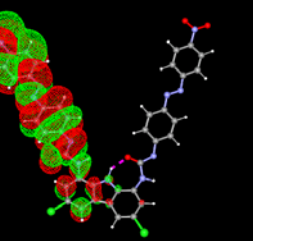
## VI. Density functional calculations

**Table S3.** TDDFT/B3LYP/6-31G* (Zindo/ B3LYP/6-31G*) calculated important transitions for **1** and **1**-CH$_3$COO$^-$ complex.



| **1** 5th HOMO (202) | **1** 2nd HOMO (205) | **1** LUMO (207) | **1** 2nd LUMO (208) |
|---|---|---|---|

205 => 208, 3.15eV, **394** nm, f=1.43; 202 => 207, 3.07eV, **403** nm, f=0.42; average = **398.5** nm
[Zindo//B3LYP/6-31G*: 132 => 136 (LUMO), 401 nm, f=2.11; 133 => 137 (2$^{nd}$ LUMO), 413 nm f=0.53]



| **1**-CH$_3$COO$^-$ 4$^{th}$ HOMO (219) | **1**-CH$_3$COO$^-$ HOMO (222) | **1**-CH$_3$COO$^-$ LUMO (223) | **1**-CH$_3$COO$^-$ 2$^{nd}$ LUMO (2224) |
|---|---|---|---|

219 ->224, 2.68eV, 462 nm, f=0.62; 219 =>223, 2.65eV, 467 nm, f=0.50
[Zindo//B3LYP/6-31G*: combined with many transitions, 465 nm  f=1.75, 475 nm, f=1.06]
Experimental : 495(shoulder)-445
Red shift : Experiment : 27 nm, Theoretical prediction: ~60 nm
The theoretical prediction shows overestimation in the red shift of the absorption peak of **1** upon binding with CH$_3$COO$^-$. However, it is conceivable that upon binding with CH$_3$COO$^-$, the electron density of the (4-nitro-phenyl)-phenyl-diazene increases with the increased electron density on the nitro-phenyl on the 1$^{st}$ and 2$^{nd}$ LUMO excited states. This increase in the electron density in the LUMO states of the color moiety leads to the red-shift upon binding of **1**with various anions.

**Table S4.** TD/B3LYP/6-31G* ([#]Zindo/ B3LYP/6-31G*) calculated important transitions for **1**-OH complex and **1**⁻.

| TD//B3LYP/6-311+G* | | | |
|---|---|---|---|
|  |  |  |  |
| **1**-2OH⁻<br>2nd HOMO (214) | **1**-2OH⁻<br>HOMO (216) | **1**-2OH⁻<br>LUMO (217) | **1**-2OH⁻<br>2nd LUMO (218) |
| 214 =>217, 2.26eV, **549** nm, f=1.07; 216 =>218, 1.95eV, **637** nm, f=0.51; average = **593** nm<br>[Zindo//B3LYP/6-31G*: 142 =>144(LUMO), 607 nm, f=2.83; 143=>145, 654 nm, f=0.76; average= 630.5 nm] | | | |
|  |  |  |  |
| **1**²⁻<br>2nd HOMO (205) | **1**²⁻<br>HOMO (206) | **1**²⁻<br>LUMO (207) | **1**²⁻<br>2nd LUMO (208) |
| 205 =>207, 1.98eV; 625 nm, f=0.45; 205 =>208+206=>208, 2.05eV, 605 nm, f=0.52; 205=>208, 2.16eV, 574 nm, f=0.66; average = 601 nm<br>[Zindo//B3LYP/6-31G*:135 =>137, 659 nm, f=0.99; 134 =>136(LUMO), 617 nm, f=2.71; average=638nm] | | | |
| The change in the spectral peak (nm) for the change from the neutral (**1**) to ionic form (**1**⁻):<br>Expt: **1**: 379-420 => ~620-634 nm (difference of 200-214 nm),<br>TD/B3LYP/6-31G* 394-403 => ~593-601 nm (difference of ~198 nm)<br>Zindo/B3LYP/6-31G*: 401-413 => 630-638 nm (difference of ~620-630nm) | | | |

[#]For the Zindo calculations the Cl is replaced by H, as Zindo does not have the parameters of Cl.

Hydrogen bonds, which facilitate the formation of the stable host-guest complexes during anion coordination, resulted in increased electron density of the supra-system, thereby enhancing the charge transfer from the electron deficient carbazole moiety to the electron rich azo-nitro-phenyl center. This results in increasing electron density over the azo-nitro-phenyl center. This charge transfer phenomenon led to a visible color change for most of the anions. However, the appearance of a peak at ~600 nm upon binding with the OH⁻, F⁻, succinate, and malonate was due to the deprotonation of one/two hydrogen atom(s) of the urea moieties that led to the charge transfer phenomenon from the electron rich phenyl urea anion center to the electron deficient azo-nitro-phenyl center.
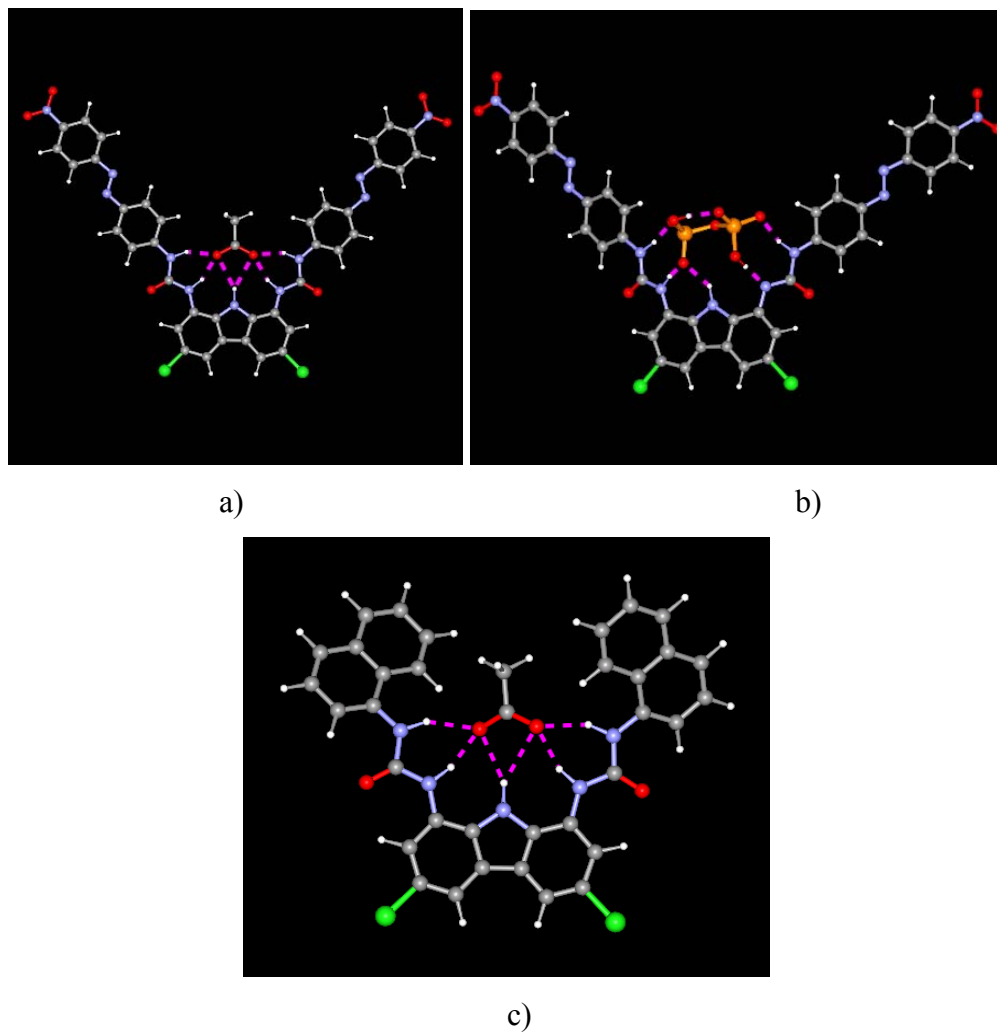
**Fig. S10.** B3LYP/6-31G* optimized geometries of complexes: a) **1**-CH$_3$COO$^-$, b) **1**-HP$_2$O$_7^{3-}$, and c) **2**-CH$_3$COO$^-$.